Protein Science (1998), 7:2511–2521. Cambridge University Press. Printed in the USA.

Crystal structure of the effector-binding domain of the trehalose-repressor of *Escherichia coli*, a member of the LacI family, in its complexes with inducer trehalose-6-phosphate and noninducer trehalose

ULRIKE HARS, REINHOLD HORLACHER, WINFRIED BOOS, WOLFRAM WELTE, AND KAY DIEDERICHS

Department of Biology, University of Konstanz, Universitätsstr. 10, 78464 Konstanz, Germany

(RECEIVED May 30, 1998; ACCEPTED August 24, 1998)

Abstract

The crystal structure of the *Escherichia coli* trehalose repressor (TreR) in a complex with its inducer trehalose-6-phosphate was determined by the method of multiple isomorphous replacement (MIR) at 2.5 Å resolution, followed by the structure determination of TreR in a complex with its noninducer trehalose at 3.1 Å resolution. The model consists of residues 61 to 315 comprising the effector binding domain, which forms a dimer as in other members of the LacI family. This domain is composed of two similar subdomains each consisting of a central β-sheet sandwiched between α-helices. The effector binding pocket is at the interface of these subdomains. In spite of different physiological functions, the crystal structures of the two complexes of TreR turned out to be virtually identical to each other with the conformation being similar to those of the effector binding domains of the LacI and PurR in complex with their effector molecules. According to the crystal structure, the noninducer trehalose binds to a similar site as the trehalose portion of trehalose-6-phosphate. The binding affinity for the former is lower than for the latter. The noninducer trehalose thus binds competitively to the repressor. Unlike the phosphorylated inducer molecule, it is incapable of blocking the binding of the repressor headpiece to its operator DNA. The ratio of the concentrations of trehalose-6-phosphate and trehalose thus is used to switch between the two alternative metabolic uses of trehalose as an osmoprotectant and as a carbon source.

Keywords: LacI family; phosphate binding; protein structure; trehalose repressor

Trehalose (Tre) is a nonreducing disaccharide consisting of two glucosyl residues with their C1-atoms linked in α,α' configuration. *Escherichia coli* is able to use extracellular Tre as a carbon source as well as to synthesize it internally as an osmoprotectant under conditions of high osmolarity (Lucht & Bremer, 1994). This requires two different metabolic pathways.

Under high osmolarity intracellular Tre is synthesized in the cytoplasm from glucose-6-phosphate and UDP-glucose (Strøm & Kaasen, 1993). Trehalose-6-phosphate (Tre6P), in this case, is an intermediate that is dephosphorylated immediately. The genes *otsA* and *otsB* encode the two enzymes catalyzing these reactions, a Tre6P-synthase and a Tre6P-phosphatase, respectively. Together, they form an operon whose expression is dependent on σ^s (RpoS), the stress sigma factor (Hengge-Aronis et al., 1991; Kaasen et al., 1992).

Under conditions of low osmolarity extracellular Tre can be taken up into the cytoplasm by a specific phosphotransferase system (PTS) (Boos et al., 1990). During the transport via the $EIIBC^{Tre}$ (TreB)/$EIIA^{Glc}$ complex, the substrate is phosphorylated to Tre6P which is released into the cytoplasm. Tre6P is hydrolysed to glucose and glucose-6-phosphate by the Tre6P-hydrolase (TreC) (Rimmele & Boos, 1994). The encoding genes *treB* and *treC* form an operon whose expression is induced by Tre6P. Tre6P is an intermediate in both the degradative and the synthetic pathways. Therefore, it is obvious that a regulation of gene expression is necessary to avoid a futile cycle.

Recently, TreR has been shown to be the repressor of the *treB/treC* operon (Horlacher & Boos, 1997). TreR is composed of 315 amino acids per monomer with the functional unit being a dimer. It binds the inducer Tre6P with a K_d of 10 μM and Tre with a K_d

Reprint requests to: Wolfram Welte, Fakultät für Biologie, Postfach 5560, M656, 78434 Konstanz, Germany; e-mail: wolfram.welte@uni-konstanz.de.

of 280 μM. Binding of Tre does not affect the repressor's affinity to its palindromic DNA operator site while Tre6P reduces its affinity. A high intracellular concentration ratio of Tre and Tre6P, as is the case under the condition of high osmolarity, displaces Tre6P from the binding site, thereby preventing the induction of the *treB/treC* operon. By this mechanism, which assumes that Tre and Tre6P bind at the same binding site of TreR, the regulation of TreR is dependent on the ratio of the concentrations of Tre6P and Tre in the cell.

In spite of this cytoplasmic switch, *E. coli* can use Tre as an energy source also under high osmotic pressure by hydrolysing it in the periplasm. A periplasmic trehalase TreA (Boos et al., 1987) is expressed under high osmotic pressure so that the glucose fragments of Tre can be taken up by the glucose transporter and metabolized.

TreR belongs to the LacI family of prokaryotic DNA-binding proteins of which more than 25 members are known that regulate the metabolism of sugars and nucleotides (Weickert & Adhya, 1992; Nguyen & Saier, 1995). This family is named after the *E. coli* lactose repressor (LacI), the protein from which the first insight into transcriptional regulation was obtained by Jacob and Monod (1961). Most members of the LacI family are dimeric, whereas LacI functions as a tetramer composed of a dimer of dimers. In most cases, transcription of the regulated operon requires the presence of an inducer molecule. In case of the *E. coli* purine repressor (PurR) (Rolfes & Zalkin, 1988) and the *Bacillus subtilis* amylase repressor (CcpA) (Henkin et al., 1991) transcription occurs in the absence of a corepressor molecule.

As master regulator of the de novo biosynthesis of purine nucleotides, PurR binds to its DNA operator site only in the presence of the corepressor molecules guanine or hypoxanthine (Choi & Zalkin, 1992). LacI binds to its operator site at the *lac* genes and downstream of the RNA-polymerase binding site in the absence of its natural inducer allolactose and thus controls the expression of enzymes coded by the *lac* operon for the degradation of β-galactosides (Jobe & Bourgeois, 1972). In addition to sugars such as allolactose and thio-β-galactosides, which act as inducers, other sugars such as lactose, glucose, phenyl β-galactoside, and orthonitrophenylfucoside bind to LacI as anti-inducers (Barkley et al., 1975) and stabilize the lac repressor–lac operator complex. Recent studies suggest that, in this complex, the binding affinity to one particular half of the operator increases (Horton et al., 1997).

The crystal structures of two members of the LacI family, PurR (Schumacher et al., 1994, 1995) and LacI (Lewis et al., 1996) have been determined both in their DNA-bound and induced forms. The structures of PurR and LacI as well as the model of the COOH-terminal domain of the *E. coli* galactose repressor (Hsieh et al., 1994) suggest that the LacI family repressor proteins share a single common fold.

They are composed of two functional domains, a 60 residue N-terminal DNA-binding headpiece containing a helix-turn-helix (HTH) motif, and a C-terminal effector binding domain (approximately 280 residues) that consists of two subdomains in a cleft between which the effector binds. In all structures the repressor protein forms dimers and the fold of the two effector binding subdomains resembles the bacterial periplasmic binding proteins, although the latter are monomers (Müller-Hill, 1983). The N-terminal DNA binding domain is not visible in the crystal structure of either PurR or LacI in the absence of operator DNA, indicating its flexibility in the unbound state. This is paralleled by the sensitivity of this domain to proteolytic cleavage as reported for LacI (Platt et al., 1973), PurR (Choi & Zalkin, 1992, 1994), and TreR (Horlacher & Boos, 1997). The crystal structures of PurR and LacI as well as the NMR structure of the DNA-binding domain of the *E. coli* fructose repressor (FruR) (Penin et al., 1997) revealed that the region between the effector binding domain and the helix-turn-helix (HTH)-motif is disordered in the absence of DNA and forms a so-called "hinge-helix" only when presented to the DNA operator site (Schumacher et al., 1994; Spronk et al., 1996). The hinge-helices of a dimer stabilize each other and participate in contacts to the DNA (Lewis et al., 1996). They are unfolded in the absence of DNA due to the lack of stabilizing α-helix N- and C-capping (Penin et al., 1997).

Structural information (Schumacher et al., 1995) as well as the analysis of more than 4,000 mutations of LacI (Suckow et al., 1996; Pace et al., 1997) revealed the mechanism of signal transduction mediated by the effector-molecule. The binding of an inducer at the interface of the two effector-binding subdomains causes a rotation of both subdomains against each other. The distance between the two NH_2-terminal DNA-binding domains thereby increases. In this nonoperator-binding conformation, the hinge helices are separated both from each other and from the DNA and are thereby destabilized. Simultaneously, the HTH motifs of the dimer are shifted apart and loose their complementary shape to the major groove of DNA; thus, the repressor's affinity for the operator drops, the repressor-operator complex dissociates, and gene transcription can take place (Schumacher et al., 1995; Lewis et al., 1996).

Here we present the crystal structure of the effector-binding domain of TreR in complexes with its inducer Tre6P and with the noninducer Tre at 2.5 and 3.1 Å resolution, respectively. We show the striking structural similarity of TreR to PurR and LacI. From this comparison, we speculate about the allosteric transition, which TreR undergoes in absence of the inducer upon binding to operator DNA.

Results

Purification and crystallization

About 40 mg pure TreR were obtained from 1 L of bacterial culture. SDS-PAGE revealed a stepwise degradation of the protein yielding a stable fragment of about 25 kD that became apparent after about 10 days. The addition of protease inhibitors did not prevent the degradation. Freezing of the protein solution for longer storage was impossible as the thawed protein precipitated. In the crystallization experiments, we therefore used up all protein within 5 days after purification. SDS-PAGE of dissolved crystals revealed the 35 kD band of the intact repressor molecule, showing that degradation was blocked in the crystals. The crystals of both complexes exhibit a hexagonal cross section and reached a size of $170 * 170 * 600$ μm^3 within 3 to 5 days. They belong to space-group $P6_5$ with cell dimensions of $a = b = 84.75$ Å, $c = 168.75$ Å and one dimer per asymmetric unit. The solvent content of the crystals is about 54%.

Structure determination of the TreR/Tre6P complex by MIR

The crystallographic data and analysis are summarized in Table 1. Useful derivatives were found with 1 mM K_2PtCl_4 and 5 mM ethylmercuriphosphate (EMP) upon soaking for 1 day. The weak phasing power up to 4 Å was much improved by collecting data at

Table 1. *Crystallographic data*[a]

Item	TreR/Tre6P					TreR/Tre
	nlocal	nESRF	nDesy	dEMP	dK_2PtCl_4	nlocal
Resolution (Å)	2.8	2.5	2.8	2.8	2.8	3.1
Obs. reflections	34,992	90,160	121,783	111,988	67,904	24,759
Unique reflections	13,615	16,376	16,084	15,986	15,908	10,017
Completeness (%)	89.0	68.6	94.5	93.9	93.4	89.1
R_{sym} (%)	14.8	8.3	11.2	10.4	11.0	17.8
R_{iso} (%)				26.9	32.1	
Phasing power up to 6.4 Å				3.47	2.22	
Phasing power up to 3.0 Å				1.18	1.2	

[a] n = Native data set; d = derivative data set.

a synchroton (DESY, Hamburg) as seen after the refinement of two strong and two weak binding sites of each derivative and inclusion of the anomalous signal (Table 1). The electron density map was improved by twofold noncrystallographic symmetry (NCS) averaging and solvent flattening. The map calculated at 3.0 Å showed clear electron density for the main chain and most of the side chains of residues 61 to 315 as well as for the inducer, so that a structural model of the effector binding domain could be built in. After two cycles of refinement resulting in an R-factor of 31.8% and an R_{free} of 33.9%, the inducer molecule was included. The model was supplemented with 22 NCS-related water molecules per monomer and was further refined in 17 cycles against the native data set nESRF. The final R-factor and R_{free} including all data up to 2.5 Å resolution were 17.3 and 21.6%, respectively. All residues are in the most favored region (92%) or the additional allowed (8%) regions of the Ramachandran plot. Standard deviations in bond lengths and angles are 0.006 Å and 1.222°, respectively (Table 2). During all refinement stages, the coordinates were strongly NCS-restrained.

Structure determination of the TreR/Tre complex

The model of the TreR determined by MIR was refined against a data set of the TreR/Tre-complex collected at a rotating anode generator with a resolution limit of 3.1 Å. The initial R-factor of 30.5% and R_{free} of 31.3% dropped after a single refinement cycle with X-PLOR including rigid body, positional and grouped B-factor refinement to an R-factor of 18.1% and an R_{free} of 23.8%.

No residues are in disallowed regions in a Ramachandran plot. The structure of the TreR/Tre complex revealed no gross conformational changes of the protein within the resolution of our analysis. Except for the missing phosphoryl group that was replaced by a water molecule, the structure is virtually identical with that of the TreR/Tre6P complex [RMS deviation (RMSD) of 0.2 Å in all carbons].

Table 2. *Refinement statistics*

	TreR/Tre6P	TreR/Tre
R_{cryst} (%)	17.3	18.1
R_{free} (%)	21.6	23.8
Number of atoms	4,022	3,970
RMSD of bond lengths (Å)	0.006	0.007
RMSD of bond angles (°)	1.222	1.262

Overall structure of the COOH-terminal domain-dimer of the TreR/Tre6P complex

The backbone structure of the effector-binding domain (residues 61 to 315, see Fig. 1) can be subdivided into two subdomains of similar topology and size (N-terminal and C-terminal). The polypeptide chain passes between both subdomains three times creating a hinge that allows rotations of the subdomains relative to each other and creating the effector binding site in their interface.

The common motif of both subdomains is a central parallel β-sheet surrounded by α-helices. The N-terminal subdomain including the residues 61 to 157 and 283 to 310 consists of six parallel β-strands in the sequence A through E and K flanked by four α-helices (I to III and X), the C-terminal subdomain including the residues 158 to 282 and 311 to 315 is composed of five parallel β-strands (F through J) flanked by six α-helices (IV to IX) (see Fig. 1).

The dimerization buries 1,600 Å^2 per monomer of the water-accessible surface. The dimerization interface is built up by helix I and strand B of the N-terminal subdomain and helices VIII and IX of the C-terminal subdomain. Intermonomeric hydrogen bonds are formed across the interface (Table 3) that are located mainly between the N-terminal subdomains. They connect the loops C-terminal of helices II and II′, as well as these loops with the peptide segment N-terminal of strand A of the other monomer, respectively. Furthermore, helices I and II are connected with strand B′ and their symmetry mates and strand B is connected with strand B′, the latter two running approximately at right angles to each other.

In the COOH terminal subdomain, Van der Waals contacts are provided by Tyr222 located on helix VI and Phe272 as part of helix IX′ and their related mates. The aromatic rings are 4 Å apart and oriented perpendicularly to each other. This arrangement has been reported to optimize electric quadrupole interaction (Burley & Petsko, 1989). The dimerization of the C-terminal subdomains is further stabilized by two hydrogen bonds between helices VIII and IX′ and their symmetry mate.

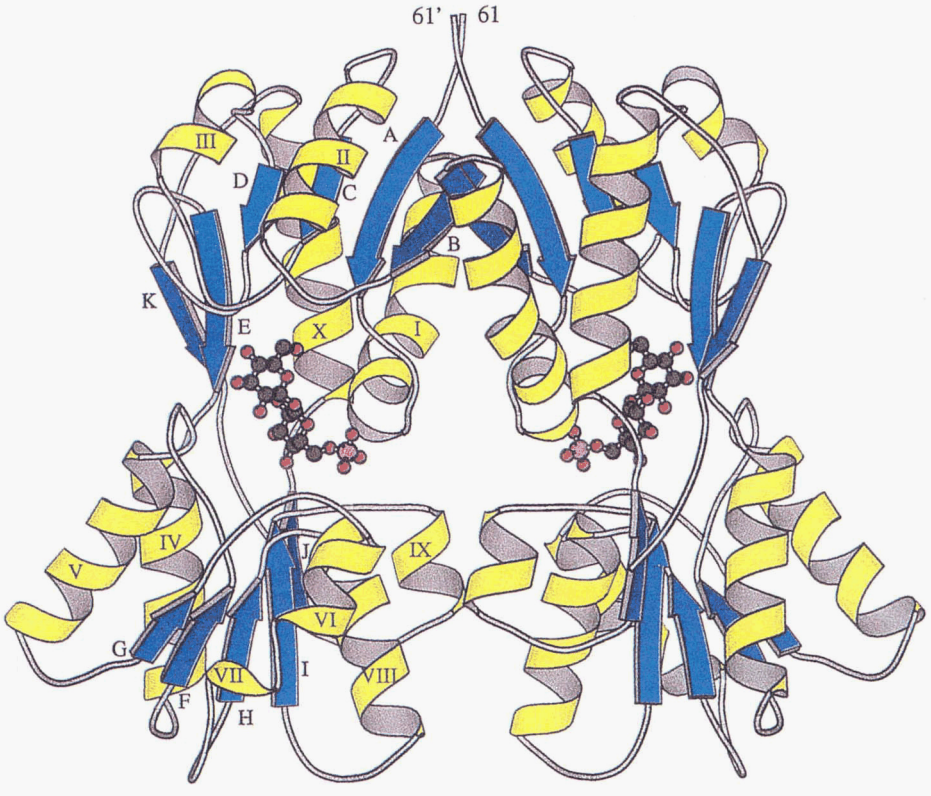

Fig. 1. Structure of the TreR effector binding domain dimer with bound inducer molecule Tre6P in ribbon representation. The β-strands are colored blue and named A through K. The α-helices are in yellow and named sequentially as I through X. The graphic was made with MOLSCRIPT (Kraulis, 1991). The N-terminal subdomain is composed of strand A (64–69), helix I (75–91), strand B (94–99), helix II (104–115), strand C (121–124), helix III (132–138), strand D (142–144), strand E (153–157), helix X (284–299), and strand K (307–310). The C-terminal subdomain consists of helix IV (159–172), strand F (178–181), helix V (192–204), strand G (210–212), helix VI (218–224), helix VII (226–228), strand H (235–238), helix VIII (241–253), strand I (260–264), helix IX (268–273), and strand J (278–281). The connecting cross-overs are at residues 157–158, 282–283, and 310–311.

The inducer binding site

The trehalose portion of the inducer molecule Tre6P is bound in a pocket where it interacts both with polar and aromatic amino acids (see Figs. 2, 3). Direct hydrogen bonds to the oxygen atoms of the sugar are provided by residues Arg71, Glu77, Gly126, Arg147, and Tyr284 of the NH_2-terminal subdomain as well as Asp187, Thr190, and Arg194 that are located in the COOH-terminal subdomain. Water mediated hydrogen bonds include Ser76, Thr189, Thr190, and Val264. The aromatic amino acids within the binding pocket are three phenylalanines, Phe102, Phe125, and Phe127, and two tyrosines, Tyr157 and Tyr284, with their aromatic rings oriented

Table 3. *Direct and water mediated hydrogen bonds across the dimer interface*

Molecule A	Molecule B	Distance (Å)	Molecule A	H_2O	Molecule B	Distance (Å)
Arg117 NE	Arg117 O	2.65	Glu99 OE1	F 18		2.83
Arg117 O	Arg117 NE	2.65		F 18	Tyr89 OH	2.94
Asp62 OD2	Arg116 NE	2.76				
Arg116 NE	Asp62 OD2	2.79	Tyr89 OH	E 18		2.92
His110 ND1	Asp94 OD1	2.81		E 18	Glu99 OE1	2.93
Asp94 OD1	His110 ND1	2.83				
Met97 O	Met97 N	2.78				
Met97 N	Met97 O	2.78				
Leu273 O	Lys249 NZ	3.10				
Lys249 NZ	Leu273 O	3.09				

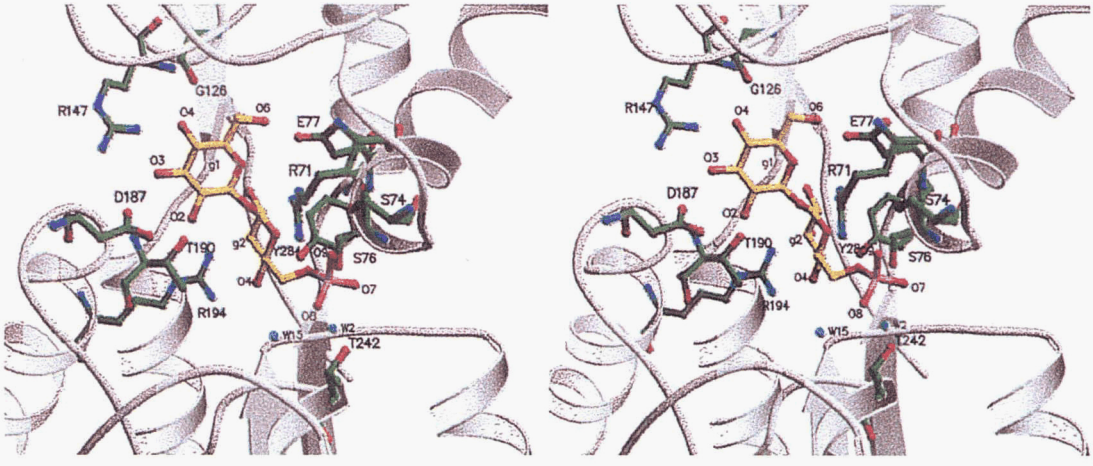

Fig. 2. Stereo view of the inducer binding site with bound Tre6P. The residues forming direct hydrogen bonds with the inducer molecule are drawn as ball-and-stick models. The orientation of the detail is similar to Fig. 1. The figure was made with MOLSCRIPT (Kraulis, 1991).

orthogonal to each other and to the sugar rings. Further hydrophobic residues within the binding pocket are Leu216 and Ala146.

While Tre is almost completely buried by the protein and has an orientation nearly parallel to α-helix X and β-strands E and K, the phosphoryl group is located at the opening of the cleft between the two subdomains. It lies between the N-termini of helix I of the N- and helix VIII of the C-terminal subdomain. Four direct and two water-mediated hydrogen bonds are formed between the phosphoryl group and the protein. Hydrogen-bond donor groups are NH1 of Arg71 and the OH group of Ser74 that form part of the loop connecting strand A and helix I, and the OH groups of Ser76 and Thr242 at the N-termini of helices I and VIII, respectively. α-Helix I is via β-strand A connected to the DNA-binding domain. The two formal negative charges of the phosphoryl group are partly compensated by the guanidinium group of Arg71, which is also linked by a salt bridge to Glu77. Water mediated hydrogen bonds are provided by Leu216 and Thr240 from the C-terminal subdomain.

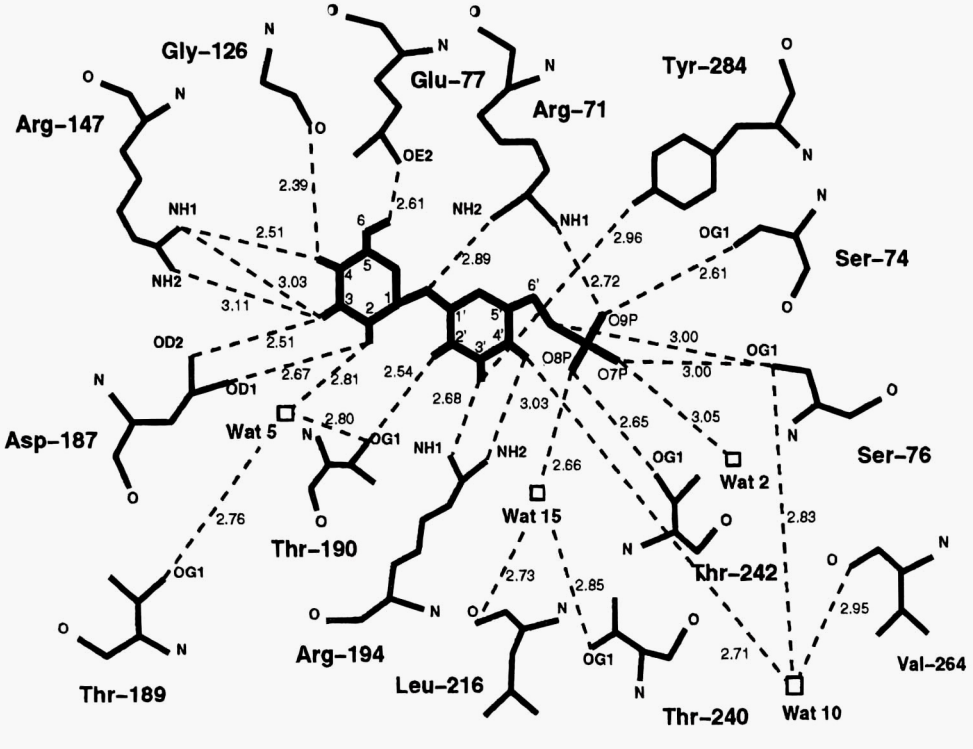

Fig. 3. Scheme of hydrogen bonds of Tre6P in its complex with TreR. The distances between acceptors and donors are given in Å.

Structural comparison of the TreR/Tre6P complex with LacI and PurR

The RMSDs at which the C_α atoms of TreR, PurR, and LacI can be superimposed (Table 4) confirm the similarity of the overall structures. The RMSDs of 1.57 and 1.93 Å, respectively, reveal a higher similarity of the monomer of the TreR/Tre6P to the PurR/corepressor/DNA complex than to the ligand free form of the PurR, indicative of a resemblance of the effector-bound conformations in spite of their opposite functions. On the other hand, the RMSD between the monomers of the TreR/Tre6P complex and LacI in the inducer-bound and apo-form is 1.73 and 2.07 Å, respectively. The structure-based sequence alignment of the effector-binding domains of TreR, PurR, and LacI (Fig. 4) reveals surprisingly low sequence identity of this domain between TreR-PurR and TreR-LacI (17.3 and 15.7%, respectively). The inducers of TreR and LacI, T6P and IPTG, respectively, as well as the corepressor hypoxanthine of PurR, differ in structure and size. Nevertheless, the amino acids taking part in hydrogen bonds to the effector molecule are conserved or lie in the same regions.

In LacI two hydrogen bonds to the inducer are provided by Arg197, which is homologous to Arg194 of TreR which binds the Tre moiety. Sequence homologies reveal this residue to be conserved in most of the members of the LacI family (Weickert & Adhya, 1992). The IPTG-binding residues Asp149 and Asp246 of LacI are almost equivalent (shifted by one residue in the structure alignment) to the effector-binding residues Arg147 and Thr242 of TreR (Fig. 4).

Other residues, which are essential for ligand binding in the three repressor structures, are located on the N-termini of helices I and V and on the preceding loops. Corepressor binding of PurR is dependent on Tyr73 and Phe74, both located at the NH_2-terminus of α-helix I in the NH_2-terminal subdomain, as well as on Arg190 in the loop before helix V, which is responsible for corepressor specificity, and Thr192, which is located at the NH_2-terminus of α-helix V in the COOH-terminal subdomain (Schumacher et al., 1994). The corresponding amino acids of TreR are Ser74, Ser76, and Glu77, lying at the NH_2-terminus of helix I, and Asp187, Thr190 as well as Arg194 that are part of a loop and the NH_2-terminal end of helix V. Of these residues only Ser74 and Ser76 form hydrogen bonds to oxygen atoms of the phosphoryl group which is responsible for induction, whereas the other residues are involved in binding of the Tre that is present in both the induced and noninduced form of TreR.

Table 4. *RMSDs of C_α atoms*[a]

	TreR/Tre6P monomer	TreR/Tre6P dimer
LacI/Ind monomer	1.729	
LacI/Ind dimer		1.965
PurR/apo monomer	1.932	
PurR/apo dimer		2.194
LacI/DNA monomer	2.073	
LacI/DNA dimer		2.323
PurR/Cor/DNA monomer	1.568	
PurR/Cor/DNA dimer		2.0

[a]Ind = inducer, Cor = corepressor, apo = without a bound effector.

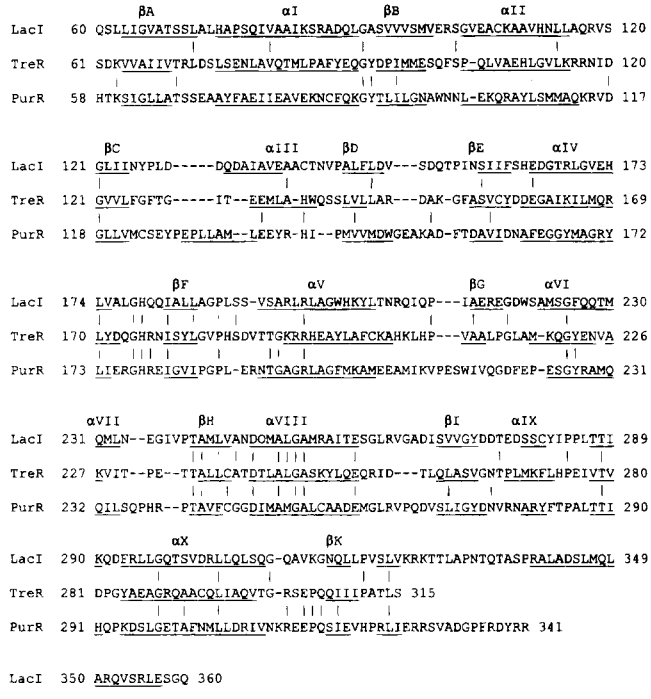

Fig. 4. Structure-based sequence alignment of TreR, LacI, and PurR. The secondary structure elements of TreR are indicated (see Fig. 1).

Discussion

Crystal structures of the TreR/Tre6P and TreR/Tre complexes

The crystal structures of TreR in complex with its inducer Tre6P and noninducer Tre, respectively, do not differ by major domain and main-chain rearrangements. Altered positions of amino acid side chains may not be recognizable due to the poor resolution limit of the TreR/Tre complex as a result of higher disorder of the crystals.

On the other hand, fluorescence measurements of Trp138 indicate structural differences between the Tre6P- and Tre-bound forms of TreR in absence of DNA (Horlacher & Boos, 1997).

This apparently contradictory observation may be explained in two ways. The structure of the TreR/Tre complex in the crystal differs from the structure in solution due to the decreased water activity caused by the high concentration of precipitant. The precipitant causes dehydration of the ligand-free phosphoryl group binding site (see below) and thus induces the conformational transition to the inducer-binding conformation, resembling the corresponding structure of LacI. Alternatively, TreR/Tre in solution may have a broad conformational variability, comprising also the crystallographically observed structure. The latter conformation could be energetically favored and thus enriched in the crystal lattice. The reduced resolution limit of the TreR/Tre crystals as compared to the TreR/Tre6P crystals is in accord with both explanations. Similarly for LacI, the crystal structures of the unliganded and inducer-bound forms are virtually identical with an

RMSD in the α-carbons of less than 0.4 Å, although they crystallized in different space groups and the former crystals were also diffracting to lower resolution than the latter (4.8 and 3.5 Å, respectively). An altered crystal structure of LacI is found only after it has been complexed with its operator DNA (Lewis et al., 1996). The DNA-binding conformation of LacI and TreR thus may be stabilized by an induced fit of the repressor to the operator.

Transcriptional regulation by ligands

In *E. coli*, Tre serves either as an osmoprotectant or as an energy source, dependent on the osmotic conditions of the medium. Because of the need to switch between the two metabolic pathways of Tre in the cytoplasm, TreR regulates the transcription of the *tre* genes by the ratio of the concentrations of Tre6P and Tre. Tre6P is the inducer, whereas Tre binds at the same binding site without reducing the aporepressor's affinity to the operator-DNA. Therefore, under in vivo conditions, either Tre6P or Tre will be bound to TreR in the inducing and DNA bound form, respectively. The phosphoryl group of Tre6P, therefore, must mediate the induction, i.e., blockage of the induced fit to the operator.

The binding site of the phosphoryl group

The phosphoryl group in the TreR-Tre6P complex contacts only two crystallographically visible water molecules so that binding must be accompanied by a considerable free energy of desolvation (Ledvina et al., 1996). The only charged residue in the neighborhood is Arg71, at a distance of 2.63 Å. There are, however, hydrogen bonds to residues of the N-terminal subdomain (the guanidinium group of Arg71 as well as two serines) and residues of the C-terminal subdomain (a Thr). The interactions with the two immobilized water molecules should also be counted as interactions with the latter subdomain.

Another structural feature is helix I whose N-terminus is in close proximity to the bound phosphoryl group. This is grossly reminiscent of the bacterial periplasmic sulfate binding protein from *Salmonella typhimurium* (SBP) in complex with a bound sulfate group (Pflugrath & Quiocho, 1985; Quiocho et al., 1987) and the corresponding phosphate-binding protein (PBP) (Luecke & Quiocho, 1990), which share topological similarity with the monomer of the TreR effector binding domain. In both binding proteins, the anion is close to the N-termini of three helices, two from one subdomain and one from the other, and the helix axes are roughly pointing toward the central anion. The oxyanion substrates are in all three cases bound with high affinity: K_D's are $\sim 10^{-6}$ M both for the sulfate and the phosphate and $0.28 \cdot 10^{-3}$ M and 10^{-5} M for Tre and its phosphate derivative, respectively. However, a closer inspection reveals that the structures of the binding sites of the phosphoryl group in TreR and from the sulfate and phosphate sites in SBP and PBP are different (see Fig. 1). Moreover, the phosphoryl group in TreR is not entirely desolvated due to the presence of two immobilized water molecules in the binding pocket.

The interaction mechanisms used in proteins for the binding of charged substrates have been a matter of debate. The idea of the macrodipole of a helix, which creates a charge pair at the distant termini of the helix resulting in a much larger potential as created by a single peptide dipole, has been advocated (Hol et al., 1978). This potential, however, predicted unrealistically large contributions to the binding energy (Åqvist et al., 1991). Quiocho et al. (1987) therefore directed attention toward arrays of hydrogen bonds in the binding site, and proposed that by their dipolar nature and their suitable arrangement around the ion they allow for favorable binding by screening the electric field of the bound ion. In SBP and PBP most of the hydrogen bonds are provided by backbone atoms. The negative potential of the dianion in their view shifts the peptide bond structure toward its deprotonated, charged, limiting structure. This shift polarizes successive peptide groups of the array and thereby increases the interaction energy with the ion. An α-helix in this explanation provides three parallel in tandem hydrogen-bond arrays along its axis.

The conclusion of these authors is that the protein allows for tight binding of ions by substituting the water of solvation by a system of hydrogen bonds in the binding pocket (Warshel et al., 1989).

Åqvist et al. (1991) have calculated that only the nearest one or two in-tandem hydrogen bonds ("arrays") contribute to the electrostatic binding energy of the ion. In the case of a helix, only the two turns closest to the bound ion seem to contribute to the electrostatic binding energy. The increase in the electrostatic potential by in-tandem arrays of a hydrogen bond does not, of course, require the presence of a helix.

As the phosphate in PBP is in close neighborhood with one arginine and two aspartates and the phosphoryl group in TreR is close to Arg71, the question arises for the role of charged residues in the binding pocket (Johnson & O'Reilly, 1996). By comparing the sulfate binding pocket with the phosphate binding pocket, Luecke and Quiocho (1990) argued for a a role of charged residues in discriminating between sulfate and phosphate, i.e., for achieving high selectivity which is not required in the case of TreR.

As to the electrostatic contribution of nearby charges to the binding energy, Yao et al. (1996) and Ledvina et al. (1996) have shown that mutants of charged residues in the phosphate binding pocket show no structural changes in phosphate binding nor in affinity. The dominant contribution to the energy of binding in PBP thus comes from the hydrogen bonds, which compensate for the large, unfavorable desolvation energy. Phosphate binding sites in proteins have been reviewed by Copley and Barton (1994). Helices providing a nearby N-terminus are found in approximately 66% of all phosphate binding sites. Main-chain helical hydrogen bonding arrays in these cases often contribute the binding jointly with the apparently electrostatically favored arginines and hydrogen-bonding residues threonine and serine. There are, however, also phosphate binding sites with no helices nearby. As expected, positively charged arginines and strong hydrogen bond donors like tyrosine are responsible for the favorable interactions in these cases. The statistically obvious aptitude of the guanidinium group in arginines for interaction with phosphate groups has been justified by its molecular properties (Johnson & O'Reilly, 1996; Saenger & Wagner, 1972). On the other hand, independent of the presence of a ligand, negatively charged residues are often found at the N-terminus of helices (Richardson & Richardson, 1988).

The phosphate binding site in TreR combines all these features. We observe hydrogen bonds between the phosphoryl group and Arg71, Ser74, Ser76, Thr242 and two bound water molecules that are located at the N-terminal ends of α-helices I and VIII. Bound water molecules were also found in the PurR/guanidine complex (Schumacher et al., 1997). We assume that the binding energy accounts for the reduced flexibility of the effector binding domain as compared to the Tre-bound form and for the higher binding energy of Tre phosphate as compared to Tre. Asp73 may help to stabilize the helix N-termini pointing to the binding cleft in ab-

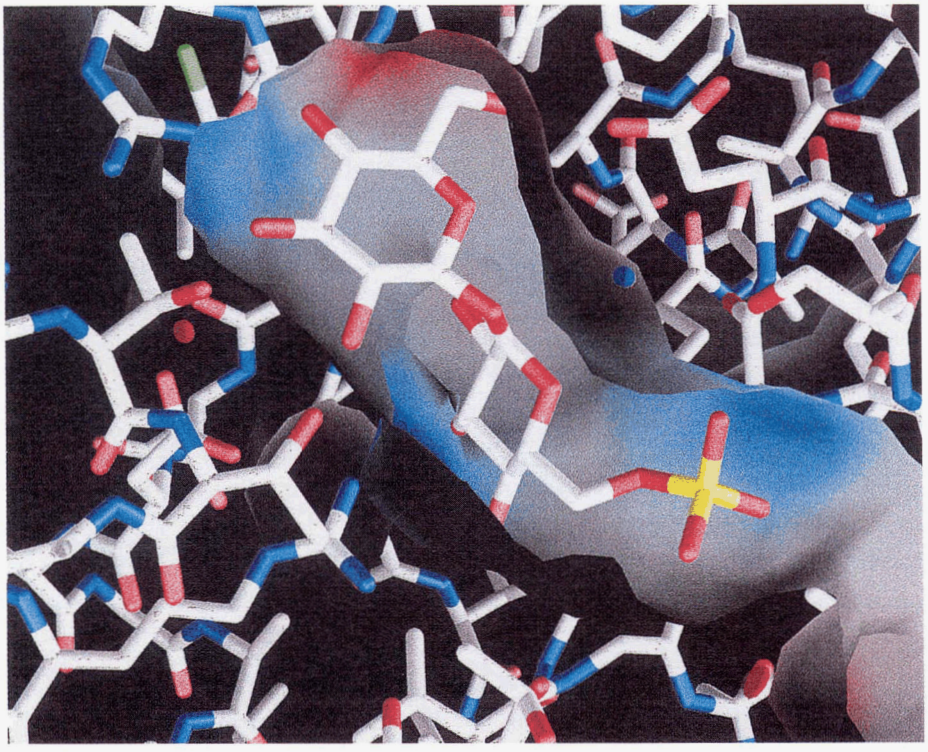

Fig. 5. Electrostatic potential on the surface of the inducer binding site in absence of Tre6P calculated with DELPHI (Honig & Nicholls, 1995) using the Poisson–Boltzmann algorithm. Blue and red surfaces represent areas of positive and negative potential, respectively. The figure was made with GRASP (Nicholls et al., 1993).

sence of the phosphoryl group (Shoemaker et al., 1987; Šali et al., 1988). An electrostatic potential calculation using the Poisson–Boltzmann approach (see Fig. 5) yields an overall positive potential in the binding cleft, a result that we think is qualitatively correct and reflects the presence of several hydrogen bonds pointing toward the binding pocket of the phosphoryl group. An unexpected negative potential was found in the phosphate binding cleft of PBP (Ledvina et al., 1996). The uniform potentials in the cleft, whether positive or negative, are caused by arrays of uniformly oriented hydrogen bond donors or acceptors that will attract water and thus will be strongly hydrated. We speculate that this pocket could be partially dehydrated at the high precipitant concentrations used for crystallization, thus shifting the conformational ensemble of the Tre-bound form toward the Tre6-P bound conformation, which resembles the inducer-bound conformation of LacI. The periplasmic binding proteins related to SBP also use their two different conformations for additional switching functions as in the case of MalE, which only in its liganded conformation creates signals for chemotaxis by binding to the Tar protein (Zhang et al., 1992) and triggers the transport process through the cytoplasmic membrane by binding to the MalF-MalG complex (Davidson et al., 1992).

The allosteric transition

As the complex of TreR with its operator is not known so far, we can only speculate about the allosteric transition, which occurs upon DNA binding by comparing with the known structures of LacI and PurR.

Both in PurR and LacI, binding to the DNA operator site induces the formation of the hinge helices (Schumacher et al., 1994, 1995; Lewis et al., 1996; Spronk et al., 1996). We assume a similar binding mode for TreR, in spite of a critical leucine being replaced by a methionine. This leucine constitutes the "leucine lever" of PurR and LacI that makes the first contact to the DNA operator site and pries the minor groove open by intercalation (Schumacher et al., 1994). It is conserved in most members of the LacI family (Weickert & Adhya, 1992). Mutational analysis of PurR showed that the substitution of a methionine for this leucine does not significantly reduce the PurR affinity to the operator DNA (Choi & Zalkin, 1994). Interestingly, PurR was found in this study to exhibit low affinity binding to nonoperator DNA. These data and others (Spronk et al., 1996) also indicate that in the non-DNA-binding conformation the hinge helix segment assumes an exposed, flexible random coil conformation. Upon encountering operator DNA, the helix-turn-helix domains of both repressor monomers bind to their sites in adjacent major grooves. Furthermore, the hinge helix forms as a consequence of the contact of the respective peptide segment with the minor groove and with its symmetry mate from the other monomer. The hinge helix dimer formation will cause a contraction of the protein between the ends of the hinge segment. We speculate that it pulls the N-terminal subdomain toward the operator especially at the edge where the dimer interface of the effector binding domain meets the headpiece dimer or, more precisely, at strand A, which is directly linked with the hinge-helical segment. This should favor the cleft opening, i.e., an increase in the distance between residues of the N-terminal subdomain and the C-terminal subdomain, which in the inducer complex are interacting with the phosphoryl group. Important for the

signal transduction between the inducer-binding domain and the DNA-binding headpiece should be helix I and strand B of TreR. In LacI they correspond to helix 5 and strand B, which also form part of the interface (Pace et al., 1997). Mutations interfering with the operator binding process in LacI have indeed found to cluster on this strand (Pace et al., 1997).

The bound noninducer Tre does not prevent the opening of the cleft and the associated rotations. We therefore think that upon opening of the cleft Tre sticks more to the N-terminal subdomain in the DNA bound form as there are more direct hydrogen bonds with this subdomain (see Fig. 3). Similarly, it is assumed for PurR that the corepressor binds to the N-terminal subdomain first, inferred from a related periplasmic binding protein (Leu-Ile-Val-binding protein) where the ligand interacts only with residues of the N-terminal subdomain when the protein is locked in its open form (Schumacher et al., 1995; Sacks et al., 1989).

In the TreR/Tre6P complex, we think that this conformational change induced by the contact with operator DNA is blocked by the interactions with the phosphoryl group which locks the N-terminal strand A and helix I to the C-terminal subunit and thus precludes movements of these structural elements within the effector-binding domains.

In the light of the data from LacI, we suggest that binding the Tre6P to DNA-bound TreR may draw the strand A/B-helix I region away from the bound DNA, the binding site cleft closes, the hinge helices loose contact to the DNA, are separated and unfolded. As a result TreR dissociates from its operator. The function of the noninducer Tre is to competitively displace the effector-molecule at high ratios of concentration of Tre/Tre6P, leaving the repressor in an operator-DNA-binding-competent conformation.

In contrast to TreR and LacI, which detach from the operator DNA upon binding of the inducer molecule, PurR binds to its specific DNA operator site only in complex with a corepressor molecule. The conformational change of the effector binding domain between the induced and DNA-bound form was examined both for PurR and LacI (Friedman et al., 1995; Schumacher et al., 1995; Lewis et al., 1996). As indicated in Results, the structure of TreR/Tre6P can be superimposed with a smaller C_α RMSD value on PurR/hypoxanthine than with its corepressor free form. In a striking similarity with PurR, the direct hydrogen bonds between the C-terminal subdomain and the ligand in TreR/Tre6P are made by residues that are part of the loop corresponding to the specificity loop of PurR and the first turn of α-helix V.

The corepressor complex of the effector-binding domain of PurR thus resembles the corresponding inducer binding complexes of LacI and TreR. The corepressor-free effector binding domain structure of PurR appears, however, to be different from the inducer-free structures of TreR and LacI.

Materials and methods

The expression system, cell growth, and purification of TreR

The expression system consists of the *E. coli* strain SF120, a protease-deficient mutant of the *E. coli* strain KS272, that is transformed with the plasmid pRHotreR. The plasmid is derived from the vector pCYTEXP1 by the insertion of *treR* into the *Nde/Eco*R restriction sites. Thereby, TreR is under control of a heat-inducible-promotor (Horlacher & Boos, 1997).

The purification protocol published by Horlacher and Boos (1997) has been changed for crystallization avoiding all precipitation steps. The cells were grown in LB-medium to an OD_{578} of 0.6 at 28 °C and induced by a fast shift to 42 °C followed by 2 h incubation at this temperature. After centrifugation at 5,000 rpm, 20 min, 4 °C, the cells were washed with buffer A (50 mM Tris/HCl, pH 7.5, 100 mM KCl, 5 mM $MgCl_2$, 1 mM DTT) and centrifuged again. Pellets were taken up in 20 mL buffer A, treated with a French Press at 16,000 psi and centrifuged at 18,000 rpm, 20 min, 4 °C. TreR was purified from the supernatant by column affinity chromatography with heparin-sepharose. The supernatant was loaded on the column with a flow rate of 1 mL/min under ice-cooling. After washing with three column bed volumes of buffer A, TreR was eluted in a linear salt-gradient from 100 (buffer A) to 500 mM KCl (buffer C, 50 mM Tris/HCl, pH 7.5, 500 mM KCl, 5 mM $MgCl_2$, 1 mM DTT). The degree of purity was examined by SDS-PAGE; the protein concentration was determined photometrically (Pace et al., 1995). An OD_{280} of 0.495 corresponds to 1 mg/mL TreR.

Crystallization

TreR was concentrated in the elution buffer using amicon-cells to 10–12 mg/mL and cocrystallized with the inducer Tre6P and non-inducer Tre, respectively, that were added in 10- and 20-fold molar excess to the protein. Crystals were grown by vapor diffusion in hanging-drops against a reservoir of 1.6 to 1.9 M Na-formiate, 0.1 M Na-acetate, pH 5.2. A drop of 22 μL of the 1:1 presaturated solution was placed on a siliconized microscope glass cover slip and equilibrated against 0.8 mL reservoir at 17 °C.

Heavy atom derivatives were prepared by soaking crystals in different concentrations of heavy atom compounds. Heavy atoms were added in small amounts from a highly concentrated aqueous stock solution to the hanging drop containing the crystals. As an initial test, the maximal concentration of the heavy atom compound was determined at which the crystals did not crack. Using this concentration the soaking time was varied between 2 h to 2 days before mounting the crystal.

Data collection and reduction

Crystals were mounted in glass capillaries (0.7 mm) and fixed vertically on a goniometer head. Data collection at a home based rotating anode X-ray generator [CuK, 100 mA, 40 kV, graphite monochromator (Schneider, Offenburg, Germany)] and an image plate detector system (STOE, Darmstadt, Germany) was performed with a rotation angle of 0.5° and an exposure time of 20 min per frame. During the measurements the crystals were cooled by an air-jet crystal cooler (FTS, New York, New York) to 4 °C. Due to radiation damage the position of each crystal in the beam was shifted along its long axis after about 20° of rotation.

A native data set of the TreR/Tre6P complex was collected at ESRF in Grenoble (beam line BL19, λ = 0.905 Å, 1 min per frame, 0.3° rotation angle), native and derivative data sets of the TreR/Tre6P complex were collected at DESY in Hamburg (beam line EMBL X11, λ = 0.89 Å, 1 min per frame, 0.5° rotation angle). All data were reduced with the program XDS (Kabsch, 1988).

Initial phases determination by multiple isomorphous replacement (MIR)

Native and derivative data sets were scaled and difference Patterson maps were calculated with the program XtalView (McRee, 1993). Heavy atom refinement and phasing were done using the program DAREFI (Dickerson et al., 1968) with inclusion of the

anomalous signal. The initially calculated electron density was improved by molecular averaging and solvent flattening with the program DM from the CCP4 package. In the resulting MIR electron density map, a polyalanine chain could be built with the BONES-option of the program O (Jones & Kjeldgaard, 1995). After replacing the alanines with the sequence of TreR, the atomic coordinates of the model were refined with X-PLOR (Brünger, 1992) and after each cycle of refinement two $F_{obs} - F_{calc}$ electron density and $F_{obs} - F_{calc}$ difference electron density maps were calculated. During all refinement stages, the coordinates were strongly NCS-restrained. Partial rebuilding of the model to receive an improved fit to the electron density was done manually at the beginning of each cycle of refinement in the program O on a Silicon graphic workstation.

Tre6P was built in the electron density composed of the structures of glucose and glucose-6-phosphate that were received from the molecular data bank creating a topology file for the complete Tre6P by the program XPLO2D Kleywegt (1995). The stereochemistry of the final model was examined by ProCheck (Laskowski et al., 1993).

Acknowledgments

This work was supported by the Deutsche Forschungsgemeinschaft. The coordinates are deposited in the Brookhaven Protein Data Bank (1BYK). We are grateful to Dr. Jason Breed for his useful comments about the manuscript and to Synchrotron staff at the ESRF and EMBL.

References

Åqvist J, Luecke H, Quiocho FA, Warshel A. 1991. Dipoles localized at helix termini of proteins stabilize charges. *Proc Natl Acad Sci USA 88*:2026–2030.

Barkley MD, Riggs AD, Jobe A, Bourgeois S. 1975. Interaction of effecting ligands with *lac* repressor and repressor-operator complex. *Biochemistry 14*:1700–1712.

Boos W, Ehmann U, Bremer E, Middendorf A, Postma P. 1987. Trehalase of *Escherichia coli* mapping and cloning of its structural gene and identification of the enzyme as a periplasmic protein induced under high osmolarity growth conditions. *J Biol Chem 262*:13212–13218.

Boos W, Ehmann U, Forkl H, Klein W, Rimmele M, Postma P. 1990. Trehalose transport and metabolism in *Escherichia coli*. *J Bacteriol 172*:3450–3461.

Brünger AT. 1992. *X-PLOR version 31: A system for X-ray crystallography and NMR*. New Haven, CT: Yale University Press.

Burley SK, Petsko GA. 1989. Electrostatic interactions in aromatic oligopeptides contribute to protein stability. *TIBTECH 7*:354–359.

Choi KY, Zalkin H. 1992. Structural characterization and corepressor binding of the *Escherichia coli* purine repressor. *J Bacteriol 174*:6207–6214.

Choi KY, Zalkin H. 1994. Role of the purine repressor hinge sequence in repressor function. *J Bacteriol 176*:1767–1772.

Copley RP, Barton GJ. 1994. A structural analysis of phosphate and sulfate binding sites in proteins. *J Mol Biol 242*:321–329.

Davidson AL, Shuman HA, Nikaido H. 1992. Mechanism of maltose transport in *Escherichia coli*: Transmembrane signaling by periplasmic binding proteins. *Proc Natl Acad Sci USA 89*:2360–2364.

Dickerson RE, Weinzierl JE, Palmer RA. 1968. A least-squares refinement method for isomorphous replacement. *Acta Cryst B42*:997–1003.

Friedman AM, Fischmann TO, Steitz, TA. 1995. Crystal structure of lac repressor core tetramer and its implications for DNA looping. *Science 268*:1721–1727.

Hengge-Aronis R, Klein W, Lange R, Rimmele M, Boos W. 1991. Trehalose synthesis genes are controlled by the putative sigma-factor encoded by *rpoS* and are involved in stationary-phase thermotolerance in *Escherichia coli*. *J Bacteriol 173*:7918–7924.

Henkin TM, Grundy FJ, Nicholson WL, Chambliss GH. 1991. Catabolite repression of alpha-amylase gene expression in *Bacillus subtilis* involves a trans-acting gene product homologous to the *Escherichia coli lacI* and *galR* repressors. *Mol Microbiol 5*:575–584.

Hol WGJ, van Duijnen PT, Berendsen HJC. 1978. The α-helix dipole and the properties of proteins. *Nature 273*:443–446.

Honig B, Nicholls A. 1995. Classical electrostatics in biology and chemistry. *Science 268*:1144–1149.

Horlacher R, Boos W. 1997. Characterisation of TreR, the major regulator of the *Escherichia coli* trehalose system. *J Biol Chem 272*:13026–13032.

Horton N, Lewis M, Lu P. 1997. *Escherichia coli* lac repressor-lac operator interaction and the influence of allosteric effectors. *J Mol Biol 265*:1–7.

Hsieh M, Hensley P, Brenowitz M, Fetrow JS. 1994. A molecular model of the inducer binding domain of the galactose repressor of *Escherichia coli*. *J Biol Chem 269*:13825–13835.

Jacob F, Monod J. 1961. Genetic regulatory mechanisms in the synthesis of proteins. *J Mol Biol 3*:318–356.

Jobe A, Bourgeois S. 1972. *lac* Repressor-operator interaction VI the natural inducer of the *lac* operon. *J Mol Biol 69*:397–408.

Johnson LN, O'Reilly M. 1996. Control by phosphorylation. *Curr Op Struct Biol 6*:762–769.

Jones TA, Kjeldgaard M. 1995. *Manual for O version 5.10*.

Kaasen I, Falkenberg P, Styrvold OB, Strøm AR. 1992. Molecular cloning and physical mapping of the otsBA genes, which encode the osmoregulatory trehalose pathway of *Escherichia coli*. Evidence that transcription is activated by KatF (AppR). *J Bacteriol 174*:889–898.

Kabsch W. 1988. Evaluation of single-crystal X-ray diffraction data from a poition-sensitive detector. *J Appl Cryst 29*:916–924.

Kleywegt GJ. 1995. Dictionaries for heteros ESF/CCP4. *Newsletter 31*:45–50.

Kraulis P. 1991. MOLSCRIPT: A program to produce both detailed and schematic plots of protein structures. *J Appl Crystallogr* 24:946–950.

Laskowski RA, MacArthur MW, Thornton JM. 1993. PROCHECK: A program to check the stereochemical quality of protein structures. *J Appl Cryst 26*:283–291.

Ledvina PS, Yao N, Choudhary A, Quiocho FA. 1996. Negative electrostatic surface potential of protein sites specific for anionic ligands. *Proc Natl Acad Sci USA 93*:6786–6791.

Lewis M, Chang G, Horton NC, Kercher MA, Pace HC, Schumacher MA, Brennan RG, Lu P. 1996. Crystal structure of the lactose operon repressor and its complexes with dna and inducer. *Science 271*:1247–1254.

Lucht JM, Bremer E. 1994. Adaptation of *Escherichia coli* to high osmolarity environments: Osmoregulation of the high-affinity glycine betaine transport system ProU. *FEMS Microbiol Rev 14*:3–20.

Luecke H, Quiocho FA. 1990. High specificity of a phosphate transport protein determined by hydrogen bonds. *Nature 347*:402–406.

McRee DE. 1993. *Practical protein crystallography*. New York: Academic Press, Inc.

Müller-Hill B. 1983. Sequence homology between Lac and Gal repressors and three sugar-binding periplasmic proteins. *Nature 302*:163–164.

Nguyen CC, Saier MH Jr. 1995. Phylogenetic, structural and functional analyses of the LacI-GalR family of bacterial transription factors. *FEBS Lett 377*:98–102.

Nicholls A, Bharadwaj R, Honig B. 1993. GRASP graphical representation and analysis of surface properties. *Biophys J 64*:A166.

Pace HC, Kercher MA, Lu P, Markiewicz P, Miller JH, Chang G, Lewis M. 1997. Lac repressor genetic map in real space. *TIBS 22*:334–339.

Pace NC, Vajdos F, Fee L, Grimsley G, Gray T. 1995. How to measure and predict the molar absorption coefficient of a protein. *Protein Sci 4*:2411–2423.

Penin F, Geourjon C, Montserret R, Böckmann A, Lesage A, Yang YS, Bonod-Bidaud C, Cortay J-C, Nègre D, Cozzone A J, Deléage G. 1997. Three-dimensional structure of the DNA-binding domain of the fructose repressor from *Escherichia coli* by ^{1}H and ^{15}N NMR. *J Mol Biol 270*:496–510.

Pflugrath JW, Quiocho FA. 1985. Sulphate sequestered in the sulphate-binding protein of *Salmonella typhimurium* is bound solely by hydrogen bonds. *Nature 314*:257–260.

Platt T, Files JG, Weber K. 1973. *Lac* repressor: Specific proteolytic destruction of the NH_2-terminal region and loss of the deoxyribonucleic acid-binding activity. *J Biol Chem 248*:110–121.

Quiocho FA, Sack JS, Vyas NK. 1987. Stabilization of charges on isolated ionic groups sequestered in proteins by polarized peptide units. *Nature 329*:561–564.

Richardson JS, Richardson DC. 1988. Amino acid preferences for specific locations at the ends of α-helices. *Science 240*:1648–1652.

Rimmele M, Boos W. 1991. Trehalose synthesis genes are controlled by the putative sigma-factor encoded by rpoS and are involved in stationary-phase thermotolerance in *Escherichia coli*. *J Bacteriol 173*:7918–7924.

Rimmele M, Boos W. 1994. Trehalose-6-phosphate hydrolase of *Escherichia coli*. *J Bacteriol 176*:5654–5664.

Rolfes RJ, Zalkin H. 1988. *Escherichia coli* gene *purR* encoding a repressor protein for purine nucleotide synthesis cloning, nucleotide sequence, and interactions with the *purF* operator. *J Biol Chem 263*:19653–19661.

Sacks JS, Saper MA, Quiocho FA. 1989. Refined X-ray structures of the leucine/isoleucine/valine-binding protein and its complex with leucine. *J Mol Biol 206*:171–191.

Saenger W, Wagner KG. 1972. An X-ray study of the hydrogen bonding in the crystalline L-arginine phosphate monohydrate complex. *Acta Cryst B 28*:2237–2244.

Šali D, Bycroft M, Fersht AR. 1988. Stabilization of protein structure by interaction of α-helix dipole with a charged side chain. *Nature 335*:740–743.

Schumacher MA, Choi KY, Lu F, Zalkin H, Brennan RG. 1995. Mechanism of corepressor-mediated specific DNA-binding by the purine repressor. *Cell 83*:147–155.

Schumacher MA, Choi KY, Zalkin H, Brennan RG. 1994. Crystal structure of LacI member, PurR, bound to DNA: Minor groove binding by helices. *Science 266*:763–770.

Schumacher MA, Glasfeld A, Zalkin H, Brennan RG. 1997. The X-ray structure of the PurR-guanine-purF operator complex reveals the contribution of complementary electrostatic surfaces and a water-mediated hydrogen bond to corepressor specificity and binding affinity. *J Biol Chem 36*:22648–22653.

Shoemaker KR, Kim PS, York EJ, Steward JM, Baldwin RL. 1987. Tests of the helix dipole model for stabilization of helices. *Nature 326*:563–567.

Spronk CAEM, Slijper M, van Boom JH, Kapstein R, Boelens R. 1996. Formation of the hinge helix in the *lac* repressor is induced upon binding to the *lac* operator. *Nature Struct Biol 3*:916–919.

Strøm AR, Kaasen I. 1993. Trehalose metabolism in *Escherichia coli*: Stress protection and stress regulation of gene expression. *Mol Microbiol 8*:205–210.

Suckow J, Markiewicz P, Kleina LG, Miller J, Kisters-Woike B, Mueller-Hill B. 1996. Genetic studies of the Lac repressor XV dag: 4000 single amino acid substitutions and analysis of the resulting phenotypes on the basis of the protein structure. *J Biol Chem 261*:509–523.

Warshel A, Åqvist J, Creighton S. 1989. Enzymes work by solvation substitution rather than by desolvation. *Proc Natl Acad Sci USA 86*:5820–5824.

Weickert MJ, Adhya S. 1992. A family of bacterial regulators homologous to gal and lac repressors. *J Biol Chem 267*:15869–15874.

Yao NY, Ledvina PS, Choudhary A, Quiocho FA. 1996. Modulation of a salt link does not affect binding of phosphate to its specific active transport receptor. *Biochemistry 35*:2079–2085.

Zhang Y, Conway C, Rosato M, Suh Y, Manson MD. 1992. Maltose chemotaxis involves residues in the N-terminal and C-termina domains on the same face of maltose-binding protein. *J Biol Chem 267*:22813–22820.